



Pembrolizumab and decitabine for refractory or relapsed acute myeloid leukemia

Meghali Goswami,^{1,2} Gege Gui,¹ Laura W Dillon,¹ Katherine E Lindblad,¹ Julie Thompson,¹ Janet Valdez,¹ Dong-Yun Kim,¹ Jack Y Ghannam ,¹ Karolyn A Oetjen,¹ Christin B Destefano,¹ Dana M Smith,³ Hanna Tekleab,¹ Yeusheng Li,¹ Pradeep Dagur,¹ Thomas Hughes,⁴ Jennifer L Marté,² Jaydira del Rivero,² Joanna Klubo-Gwiezdzinska,⁵ James L Gulley ,² Katherine R Calvo,⁴ Catherine Lai,¹ Christopher S Hourigan ^{1,6}

To cite: Goswami M, Gui G, Dillon LW, *et al*. Pembrolizumab and decitabine for refractory or relapsed acute myeloid leukemia. *Journal for ImmunoTherapy of Cancer* 2022;**10**:e003392. doi:10.1136/jitc-2021-003392

► Additional supplemental material is published online only. To view, please visit the journal online (<http://dx.doi.org/10.1136/jitc-2021-003392>).

MG and GG contributed equally.

Accepted 27 November 2021

ABSTRACT

Background The powerful ‘graft versus leukemia’ effect thought partly responsible for the therapeutic effect of allogeneic hematopoietic cell transplantation in acute myeloid leukemia (AML) provides rationale for investigation of immune-based therapies in this high-risk blood cancer. There is considerable preclinical evidence for potential synergy between PD-1 immune checkpoint blockade and the hypomethylating agents already commonly used for this disease.

Methods We report here the results of 17 H-0026 (PD-AML, NCT02996474), an investigator sponsored, single-institution, single-arm open-label 10-subject pilot study to test the feasibility of the first-in-human combination of pembrolizumab and decitabine in adult patients with refractory or relapsed AML (R-AML).

Results In this cohort of previously treated patients, this novel combination of anti-PD-1 and hypomethylating therapy was feasible and associated with a best response of stable disease or better in 6 of 10 patients. Considerable immunological changes were identified using T cell receptor β sequencing as well as single-cell immunophenotypic and RNA expression analyses on sorted CD3+ T cells in patients who developed immune-related adverse events (irAEs) during treatment. Clonal T cell expansions occurred at irAE onset; single-cell sequencing demonstrated that these expanded clones were predominately CD8+ effector memory T cells with high cell surface PD-1 expression and transcriptional profiles indicative of activation and cytotoxicity. In contrast, no such distinctive immune changes were detectable in those experiencing a measurable antileukemic response during treatment.

Conclusion Addition of pembrolizumab to 10-day decitabine therapy was clinically feasible in patients with R-AML, with immunological changes from PD-1 blockade observed in patients experiencing irAEs.

INTRODUCTION

Acute myeloid leukemia (AML) is an oligoclonal hematological malignancy characterized by myeloid leukemic blasts in the bone marrow (BM) and peripheral blood (PB).

The majority of patients diagnosed with AML will develop relapsed or refractory disease (R-AML). Response rates to intensive salvage therapy for AML patients who relapse range from 30% to 50%, while response rates for those with refractory disease are even lower, typically under 10%.^{1,2} There is no standard of care for adult R-AML other than referral to an appropriate clinical trial. The graft-versus-leukemia effect of allogeneic hematopoietic cell transplantation for AML provides precedent for the investigation of other immunotherapeutic approaches to treat R-AML. The anti-leukemic benefit of such transplants however is balanced by the risk of severe immunological toxicity against recipient host tissues.^{3,4}

Immune checkpoint blockade (ICB) of the PD-1 signaling axis has proven to be one of the most important advances in cancer treatment.⁵ The PD-1 immunoreceptor has two known ligands (PD-L1 and PD-L2); binding of either ligand to PD-1 attenuates T cell receptor (TCR) signaling. Persistent antigenic stimulation can lead to sustained PD-1 expression and T cell dysfunction or exhaustion.^{6,7} T cell exhaustion is prevalent in many cancers, and therapeutic monoclonal antibodies against PD-1 can abrogate T cell exhaustion and restore functionality.^{8–11}

Seminal murine studies demonstrated a role for PD-1/PD-L1 blockade in the reduction of AML tumor burden.^{12,13} We and others have shown that CD3+ T cells expressing clinically actionable inhibitory immunoreceptors, including PD-1, are present in the BM and PB of R-AML, even in those with very high burden of disease.^{14–19} Furthermore, there is biological rationale for the combinatorial use of anti-PD-1 agents and hypomethylating



© Author(s) (or their employer(s)) 2022. Re-use permitted under CC BY. Published by BMJ.

For numbered affiliations see end of article.

Correspondence to

Dr Christopher S Hourigan; hourigan@nih.gov

agents (HMAs) for R-AML with potential mechanistic synergy between these classes of drugs.²⁰ HMAs alone may cause upregulation of PD-L1/2, leading to resistance and immune escape.^{21–22} HMAs may also upregulate cancer testis antigens and reactivate previously silenced endogenous retroviruses in leukemic blasts, potentially leading to induction of tumor-specific CD8+ T cells.^{23–26} Importantly though, PD-1 is a critical mediator of peripheral tolerance, as T cells with a degree of autoreactivity upregulate PD-1 to inhibit pathogenic behavior.^{27–28} Indeed, the association between immune-related adverse events (irAEs) and ICB suggests these agents are subverting normal peripheral tolerance mechanisms, leading to autoimmune toxicities.

Pembrolizumab is a potent and highly selective humanized monoclonal antibody of the IgG₄/kappa isotype designed to directly block the interaction between PD-1 and its ligands and reinvigorate existing immune responses in the presence of antigen receptor stimulation. Decitabine is a nucleoside metabolic inhibitor that directly incorporates into DNA and inhibits DNA methyltransferase, causing hypomethylation of DNA and cellular differentiation or apoptosis. Decitabine is commonly used for standard of care treatment of AML.^{29–30}

Here, we report outcomes of the first clinical trial (NCT02996474) to investigate the novel combination of pembrolizumab and decitabine in R-AML. In addition, to explore potential induced immunological changes during treatment, we used TCR β DNA-sequencing (TCR β -seq) on serial samples to construct a picture of clonotypic T cell dynamics during treatment. We then used single-cell RNA sequencing (scRNA-seq) with full length TCR sequencing and cell surface antibody-oligonucleotide staining to understand immunogenomic and phenotypic changes associated with the important clinical outcomes of toxicity and efficacy observed in the trial.

MATERIALS AND METHODS

Clinical trial

Pembrolizumab 200 mg was administered intravenously on day 1 of every 3-week cycle, with decitabine 20 mg/m² administered on days 8–12 and 15–19 (ie, total of 10 days) of alternative cycles starting with cycle 1. Up to eight cycles (24 weeks) of therapy were given, with the opportunity for an optional continuation phase for those who maintained a best response of at least stable disease after the initial planned eight cycles. Patients were adults with an unequivocal diagnosis of R-AML confirmed by an NIH attending pathologist within 30 days of study enrollment. Those with acute promyelocytic leukemia, prior allogeneic hematopoietic stem cell transplant, active autoimmunity or second malignancy, prior PD-1 axis inhibitor therapy or more than two cycles of prior decitabine therapy were excluded from participation. Full eligibility, response and discontinuation criteria are reported in online supplemental table S1.2. BM examinations for clinical response assessment were performed

prior to treatment and after cycles 2, 4, 6 and 8 (or the progression/off-study time-point). An additional BM examination was performed for research purposes on day 8 of the first cycle (ie, 1 week after the first dose of pembrolizumab, immediately before the initiation of decitabine).

Sample collection

BM aspirate and PB was collected from enrolled patients. A cohort of healthy donors (HD, n=13) was also recruited as a control population at the NIH; we previously intensively characterized the BM of this cohort with scRNA-seq, flow cytometry, and immunohistochemistry of BM core biopsies.^{15–31} BM mononuclear cells (BMMCs) were purified from BM aspirate using density centrifugation, cryopreserved, and stored in liquid nitrogen. CD8+ T cells were enriched from thawed BMMCs with CD8 positive microbeads according to manufacturer's protocol (Miltenyi Biotec).

Nucleic acid isolation

Genomic DNA (gDNA) was isolated from 2 mL of fresh heparinized BM and 2 mL of PB using DNA Blood Midi Kits (Qiagen) according to manufacturer's instructions. AllPrep RNA/DNA Mini Kits (Qiagen) were used to isolate gDNA from CD8+ T cell populations enriched from BMMCs. All gDNA was quantitated using both absorbance (NanoDrop, Thermo Fisher) and fluorometric (Qubit, Thermo Fisher) methods.

Bulk TCR β sequencing and TCR data analyses

The complementarity-determining region 3 (CDR3) region of rearranged TCR β genes was sequenced using the survey depth immunosequencing platform from Adaptive Biotechnologies. Target gDNA input from BM and PB samples was 1–2 μ g, and the entire gDNA yield from sorted CD8+ T cells was input into the sequencing assay. Amplification and sequencing of the TCR β CDR3 was performed according to previously described protocols,^{32–33} and sequenced regions were filtered, mapped, and defined according to the IMGT database.³⁴ The ImmunoSEQ toolset from Adaptive Biotechnologies was used to explore and analyze TCR β sequencing datasets. Significantly differentially abundant T cell clones between two timepoints for a given patient were identified by employing Fisher exact statistical tests fitted with a betabinomial probability density model to account for normal variance in TCR β repertoires.^{35–36} T cell clones were considered differentially abundant if their Benjamini-Hochberg-corrected false discovery rate was less than 0.01.

Cell surface staining with oligo-tagged antibodies and enrichment of CD3+ T cells

To purify CD3+ T cells from cryopreserved BMMCs from AML patients, frozen cells were thawed into warmed 37°C RPMI-1640 supplemented with 50% fetal bovine serum (FBS), washed twice, and counted with trypan blue staining on an automated hemocytometer. Between

500 000 to 1 million cells were resuspended in 56 μ L of RPMI-1640 with 10% FBS, to which 5 μ L of TruStain FcX and 2 μ L of a 1:1 weight to volume solution of dextran sulfate was added. Cells were incubated with the FcX block and dextran for 10 min at room temperature (RT), after which 10 μ L of FITC-conjugated anti-human CD3 (clone HIT3a, Biolegend) and 0.5 μ g each of the 27 TotalSeq-C oligo-tagged antibodies (Biolegend) listed in online supplemental table S3 were added. Cells were incubated with antibodies for 30 min at RT in the dark. After incubation, cells were washed twice with RPMI-1640 with 10% FBS and resuspended in 300 μ L of the same buffer. Five minutes prior to the start of fluorescence-activated cell sorting (FACS) acquisition, 2 μ L of a 1 mg/mL DAPI live dead stain (Thermo Fisher Scientific) was added to the cell suspension, and cells were filtered through 40 μ m cell strainers immediately prior to acquisition. FACS was performed using a BD Aria II equipped with Diva software. After debris and doublet exclusion, live CD3+ T cells were sorted into RPMI-1640 with 10% FBS using a 100 μ m nozzle instead of the standard 20 μ m nozzle, reducing the pressure per cell from 70 psi to 20 psi during the sorting process. A minimum of 10,000 live T cells were sorted. Immediately after sorting, samples were centrifuged at 250 \times g for 5 min using a swing-arm rotor centrifuge, and volume was adjusted so estimated cell concentration based on cell number sorted was 1000–2000 cells/ μ L. Cell concentration was verified using trypan blue stain on an automated hemocytometer.

5' scRNA-seq library construction and sequencing

The 10x Genomics 5' Single Cell Immune profiling platform was used for scRNA-seq of enriched T cells. After FACS of oligo-stained CD3+ T cells, the cells were loaded on a Chromium Chip with master mix, gel beads, and partitioning oil according to manufacturer's instructions. Intended number of cells captured was 6000–8000. Reverse transcription of mRNA into barcoded first strand cDNA, as well as construction of gene expression (GEX), VDJ, and antibody-derived tag (ADT) sequencing libraries was performed according to the experimental protocol and reagents provided by 10x Genomics, without modifications. GEX, VDJ, and ADT libraries were evaluated using an Agilent TapeStation and quantitated with qPCR (Kapa). The scRNAseq libraries were pooled and sequenced with an Illumina NovaSeq S4 flow cell using an Xp loader. Libraries were sequenced PE28-8-98 with 1% PhiX. Target sequencing depth for the GEX libraries was 20,000 read pairs per cell and 5000 read pairs per cell for the VDJ and ADT libraries.

5' scRNA-seq data processing and analyses

5' sequencing libraries were preprocessed using Cell Ranger V.3.1.0 (10x Genomics) to obtain GEX, feature barcoding counts, and VDJ information. The number of barcode mismatches was set to be 0 to minimize the demultiplexing error. Seurat v3 was used across the study for sample basic quality control, normalization, data

integration, visualization, and differential expression. Default methods were used unless otherwise specified for specific tasks. Data from all samples were integrated for visualization using the standard workflow on Seurat v3 by identifying the anchors between individual samples using the top 2000 variable genes within each and reducing dimensions by principal component analyses then uniform manifold approximation and projection. Immunophenotyping of the cells was analogous to flow cytometry where raw counts of marker proteins including CD3, CD45, CD4, CD8, CD127, CD25, CCR7, and CD45RA were plotted, and consensus cutoffs were created by comparing median cutoffs across different timepoints within one sample and adjusting them across all patients.

3' scRNA-seq library construction and sequencing

The 10x Genomics 3'v3 Single Cell Immune profiling platform was used for scRNA-seq of BMMCs. Frozen cells were thawed as described earlier, with the addition of a wash step with 5 mL of ACK lysis buffer to lyse any residual red blood cells. Up to 1 million cells were resuspended in 50 μ L of cell labeling buffer (PBS+1% BSA). Cells were incubated with TruStain FcX (Biolegend) for 10 min at 4C, after which 0.5 μ g each of the 46 TotalSeq-A oligo-tagged antibodies (Biolegend) listed in online supplemental table S4 were added. Cells were incubated with antibodies for 30 min at RT at 4C. After incubation, cells were washed three times with cell labeling buffer and filtered with 40 μ m Flowmi cell strainers. Final volumes were adjusted so estimated cell concentration was 700–1200 cells/ μ L using trypan blue stain on an automated hemocytometer. Oligo-tagged cells were loaded on a Chromium Chip B with master mix, gel beads, and partitioning oil, again according to 10x Genomics instructions. cDNA amplification was performed according to manufacturer's instructions with the addition of 1 μ L 0.2 μ M ADT additive primer (online supplemental table S5) per sample to amplify ADT tags. During cDNA cleanup, supernatant containing the ADT cDNA fraction was kept and used for generation of ADT libraries. Two rounds of 2X ADT cDNA purification were performed with SPRIselect beads, and 100 μ L PCR reactions for library preparation and amplification were prepared by mixing 2.5 μ L of purified ADT cDNA fraction with 2.5 μ L of 10 μ M SI PCR primer, 2.5 μ L 10 μ M Illumina TruSeq small RNA RPI primer, 50 μ L 2X Kapa Hifi PCR master mix, and 50 μ L RNase-free water. All primer sequences for ADT library generation are detailed in online supplemental table S5. Reactions were amplified in a thermocycler at 98C for 2 mins, then 14 cycles of 98C for 20s, 60C for 30s, and 72C for 20s, followed by 5 min at 72C. The amplified ADT libraries were purified with 1.2X SPRIselect beads. 3'v3 GEX libraries were constructed exactly according to 10x Genomics protocol. 3'v3 GEX and ADT libraries were evaluated as earlier described, and scRNAseq libraries were pooled and sequenced with an Illumina NovaSeq SP flow cell using an Xp loader. Libraries were sequenced PE28-8-98 with

1% PhiX. Target sequencing depth for the GEX libraries was 20 000 read pairs per cell and 5000 read pairs per cell for the ADT libraries.

3'v3 scRNA-seq data processing and analyses

The standard pipeline for Cell Ranger version 3.1.0 (10x Genomics) was used to obtain unique molecular identifier (UMI) counts for GEX and cell surface antibodies. The number of barcode mismatches was set to 0 to minimize demultiplexing error. Seurat v3 was used for sample basic quality control, normalization, visualization, and differential expression. Each sample was analyzed individually, and clustering was performed based on normalized cell surface protein expression. Highly expressed proteins were identified for cell type annotation and leukemia associated clusters were labeled based on markers from previous clinical flow cytometry records.

scDNA-seq library construction, sequencing, and analysis

The MissionBio Tapestry scDNA-seq V2 platform with antibody-oligonucleotide staining was performed on BMMCs per manufacturer's protocol. Custom primers targeting patient-specific mutations and chromosomal abnormalities, as well as oligonucleotide antibodies against CD45, CD34, CD117, CD11b, CD123, CD13, CD33, CD38, CD90, CD7, CD3, CD19, HLA-A,B,C, HLA-DR, and HLA-DR, DP, DQ were used in this assay. All experimental acquisition, library generation, sequencing, data processing, and analyses were performed exactly as previously described.³⁷

Statistical analyses

GraphPad Prism (V.8.4.3) and R V.4.0.0 were used for statistical analyses and graphing. Several R packages (ggplot2, Seurat, pheatmap) were used for data manipulation and visualization. This work utilized the computational resources of the NIH HPC Biowulf cluster (<http://hpc.nih.gov>).

RESULTS

Safety and efficacy of pembrolizumab with decitabine in R-AML

Ten high-risk previously treated adult R-AML patients (median age 62, range 30–81) were enrolled in the clinical trial 17H-0026 (PD-AML, 17H-0026, NCT02996474) between March and November 2017 at the NIH Clinical Center. The treatment schema and research sampling intervals are shown in [figure 1A](#). At enrolment seven patients had refractory disease (including two with therapy-related myeloid neoplasms) and three had early relapse within 6 months from completion of last therapy ([figure 1B](#)). Five patients had received prior HMA treatment. The primary study aim was to determine feasibility of this novel treatment combination; evaluation of safety and efficacy were additional clinical objectives.

The median number of pembrolizumab doses administered was 6 (mean: 5.8, range 3–8) of a possible 8. The

median number of cycles of 10-day decitabine was 3.75 (mean: 3.1, range 1.5–4). The median overall survival from the first day of study treatment was 10 months (mean: 10.8 months, range 2.4–24.6 months) ([figure 1C](#)). No grade 5 adverse events occurred; most grade 4 adverse events were hematological. Non-hematological grade 4 events (sepsis) were seen in two subjects. The toxicity profile of this novel combination therapy was largely consistent with that expected from decitabine alone with the exception of three patients who suffered irAEs likely as a consequence of pembrolizumab ([figure 1D](#)). This included 2 patients developing hypothyroidism (after 2 and 4 cycles respectively) and a third diagnosed with central diabetes insipidus (after four cycles).

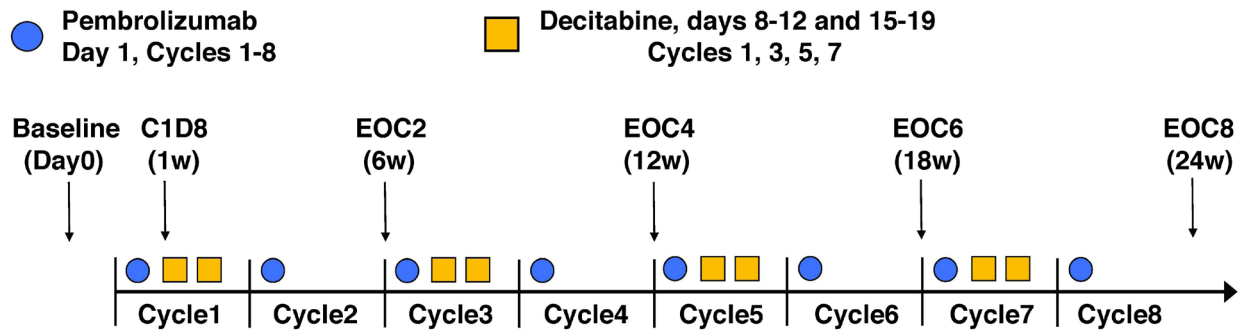
In summary, 4 of 10 patients had leukemic progression prior to cycle 8 and were taken off study per protocol rules (online supplemental figure S1). An additional patient was taken off study due to grade 4 infection in cycle 5 while in a morphological leukemic free state (MLFS). For those completing the full planned 24 weeks of the study, three had stable disease and two were in a cytomorphological complete remission (CR) including one in measurable residual disease (MRD) negative CR (online supplemental figure S1).

Specifically, a patient enrolled at second relapse achieved a CR3 lasting 337 days (compared with prior CR2 of 185 days) and was MRD negative by flow cytometry at the end of eight cycles. He survived over 15 months from the start of the protocol treatment despite having significant competing comorbidities. A patient in early first relapse had decreased blasts from 4.4% at enrolment to 0.1% at the end of eight cycles (classified as stable disease, as remained in CR with MRD) and survived over 12 and a half months from the start of protocol treatment.

Characteristic pattern of clonal T cell expansion in patients developing irAEs

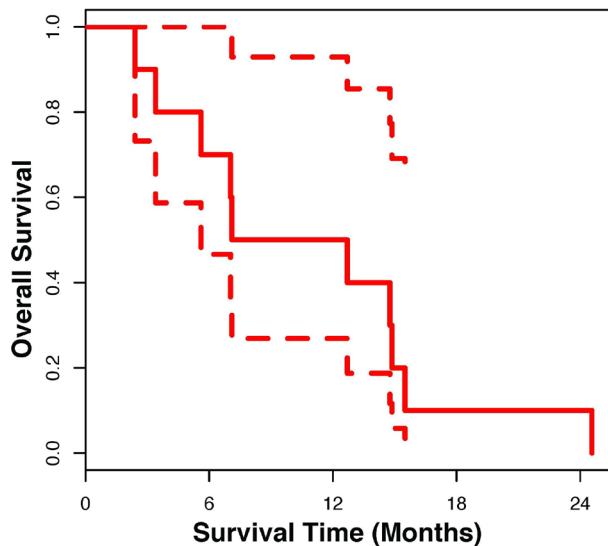
Without a randomized controlled trial, it is challenging to confidently determine if addition of anti-PD1 immunotherapy to clinical standard of care hypomethylating therapy (decitabine) is associated with increased anti-leukemic efficacy. Clinical irAEs however can be confidently attributed to the addition of this immunotherapy, allowing laboratory characterization and quantification of potentiated immune responses.

We first examined abundance and diversity of BM-infiltrating and circulating T cells across all patients and in HD of similar ages. The proportion of CD3+ T cells in the BM of AML patients prior to treatment did not differ from that of HD, in concordance with prior studies (online supplemental figure S2A).^{14 15} We noted an upward trend of CD3+ infiltrate in BM during treatment particularly in responders (online supplemental figure S2B). TCRβ sample clonality, previously reportedly as associated with response to ICB,^{38 39} as assessed by TCRβ-seq, was also within the ranges observed in HD; there was no association of baseline repertoire clonality or changes in this

A

B

Patient characteristics						
UPN	Age Range	Sex	AML Type	Prior Treatments	Day0 BM Blast %	Response at EOC8
PD-AML 1	70-79	M	Relapse	clofarabine; iDAC	5-10%	MRD negative CR
PD-AML 2	60-69	F	Refractory	7+3; EMA	10%	Stable
PD-AML 3	50-59	F	Refractory	azacytidine; 7+3	15-50%	Stable
PD-AML 4	30-39	M	Refractory	7+3; HiDAC	25-30%	n/a (progression at EOC4)
PD-AML 5	70-79	M	Relapse	7+3; iDAC	5%	Stable - CR with 0.1% MRD
PD-AML 6	50-59	F	Relapse	7+3; HiDAC	50%	n/a (progression during C3)
PD-AML 7	50-59	F	Refractory	7+3; CP + etoposide	10%	n/a (progression at EOC6)
PD-AML 8	60-69	M	Refractory	decitabine	30%	n/a (progression at EOC4)
PD-AML 9	60-69	F	Refractory	7+3; etoposide + mitoxantrone	10%	Stable
PD-AML 10	80-89	M	Refractory	azacytidine; clofarabine + velcade	10%	MLFS, no MRD at EOC5

UPN, unique patient number. iDAC, intermediate dose cytarabine. HiDAC, high dose cytarabine. EMA, etoposide + mitoxantrone + cytarabine. BM, bone marrow. MRD, measurable residual disease. CR, complete remission. MLFS, morphological leukemia-free state.

C

D

Adverse events (AEs)		
CTCAE toxicity	Grade 3	Grade 4
Platelet count decreased	0	8 (80)
Neutrophil count decreased	0	3 (30)
Febrile neutropenia	5 (50)	1 (10)
Infection / Sepsis	1 (10)	2 (20)
Lymphocyte count decreased	0	2 (20)
Hypotension	0	1 (10)
Hypophosphatemia	1 (10)	0
Hypokalemia	3 (30)	0
Blood bilirubin increased	1 (10)	0
Diarrhea	1 (10)	0
irAE	Grade 1	Grade 2
Hypothyroidism	0	2 (20)
Central diabetes insipidus*	1 (10)	0

CTCAE, common terminology criteria for AEs. irAE, immune-related AE. * thought possibly associated with pembrolizumab.

Figure 1 PD-AML clinical trial schema, sampling intervals, and survival curve. (A) Pembrolizumab was administered on day 1 of every cycle for eight cycles, and decitabine was given on days 8–12 and 15–19 of every other cycle. Bone marrow aspirate and peripheral blood was collected before the start of treatment (day 0), on cycle 1 day 8 (C1D8) after one dose of pembrolizumab, and at the end of every other cycle (EOC2, EOC4, EOC6, EOC8); clinical responses were also assessed at these timepoints. (B) Summary of patients treated on NCT02996474 and responses. These patients have been reported previously.^{37,76} (C) Kaplan-Meier survival curve with 95% CI. (D) Summary of grades 3 and 4 adverse events and irAEs that occurred during treatment. AML, acute myeloid leukemia; EOC2, end of 2 cycles of treatment; EOC4, end of 4 cycles of treatment; EOC6, end of 6 cycles of treatment; EOC8, end of 8 cycles of treatment.

measure in BM or PB with clinical response during treatment (online supplemental figure S2C-F).

As the etiology and time of clinical diagnosis of irAEs was known, we performed pairwise identification using TCR β -seq of T cell clones that significantly changed in frequency during treatment compared with baseline in patients developing irAEs. These three patients had significant clonal expansions (3–9 clones in BM and 4–15 in PB at the end of 2 cycles of treatment (EOC2), 12–40 in BM and 7–33 in PB at EOC4) (figure 2A,B). We asked whether significant expansion of T cell clonotypes from undetectable or near undetectable (<0.1% productive frequency) at baseline were temporally associated with the development of irAEs. Strikingly, we identified several clonally expanded T cells whose expansion coincided with a rise in thyroid stimulating hormone and diagnosis of hypothyroidism in patients PD-AML 2 (figure 2C) and PD-AML 9 (figure 2D). PD-AML 2 exhibited a period of thyrotoxicosis preceding overt hypothyroidism, previously described with anti-PD-1-induced thyroiditis.^{40,41} PD-AML 3, who developed central diabetes insipidus after four cycles, had pronounced CD8+ and CD4+ clonal T cell expansions that coincided with the irAE and were undetectable prior to Pembrolizumab (figure 2E). The development of irAEs were preceded by significant although temporary expansion of at least one T cell clone in all patients, and patients developing hypothyroidism continued to experience marked clonal T cell expansions one full cycle after irAE onset (online supplemental figure S3). Significantly expanded clones at irAE onset demonstrated concordant magnitudes of expansion in both BM and PB (online supplemental figure S4). These temporal associations between clonal T cell expansion after pembrolizumab and development of irAEs suggest a potential role for T cell mediated immune toxicity.

B cells are also capable of mediating autoimmunity, including Hashimoto's disease (hypothyroidism).⁴² Previously, we identified a loss of B cells in R-AML patients after chemotherapy,¹⁴ which was confirmed in this cohort of R-AML patients, including those who developed irAEs (online supplemental table S6). At irAE onset, the two patients developing hypothyroidism had normal to undetectable autoantibodies against thyroid peroxidase and thyroglobulin (online supplemental table S7). In combination, these data suggest a limited role of the humoral immune response in thyroid irAEs in these patients.

Expanded T cell clones at irAE diagnosis express activation signatures at the transcript and protein level

To understand the distinguishing immunogenomic features of individual T cells clonally expanding during the development of irAEs we next performed 5' scRNA-seq with full length VDJ TCR sequencing and cell surface antibody-oligonucleotide profiling on FACS-enriched T cells from BM (10x Genomics) from two patients experiencing irAEs (online supplemental figure S5, table S8).

All CD8+ T cell clonotypes previously identified through bulk TCR β sequencing of PD-AML 2 at the time

of diagnosis of hypothyroidism were also detected by scRNA-seq, along with paired TCR α for most clonotypes of interest. Supervised analysis of irAE-associated CD8+ T cell clonotypes compared with the ten most abundant CD8+ clones identified by TCR β -seq (all clonotypes had ≥ 5 cells with given CDR3) reveals a striking differentially expressed genes (DEG) profile (figure 3A). The majority of the irAE clonotypes expressed granulysin (*Gnly*), indicative of active cytolytic activity, high *Pdcd1* (encoding PD-1 protein), as well as genes related to T cell activation and costimulation (*Sirpg*, *Psmb8*), survival (*Coro1a*, *Pycard*), actin remodeling (*Pfn1*, *Cotla*), and metabolic reprogramming (*Ucp2*, *Gapdh*). Differentially expressed cell surface proteins (DEP) for the majority of these clones were consistent with an effector phenotype based on CCR7, CD45RA, and CD45RO (figure 3B). All expressed very high HLA-DR; the same four clones expressing *Pdcd1* transcript co-expressed cell-surface PD-1, TIM-3, and CD27, the latter suggesting recent differentiation from a more memory phenotype (figure 3B).¹⁸ The four clones sharing a common DEG and DEP signature exhibited a similar magnitude expansion in the longitudinal bulk TCR β -seq data (figure 3C). One differentially abundant clone in PD-AML 2 that was detected at baseline highly expressed *Klrc3*, suggesting an invariant NKT-like cell state for this clonotype (online supplemental figure S6A).⁴³

Using scRNA-seq in the sample acquired at time of central diabetes insipidus diagnosis for PD-AML 3, we detected the majority of expanded clonotypes including both CD8+ and CD4+ T cells. The CD8+ irAE expanded clonotypes were compared with other abundant T cells yielding an even more pronounced DEG profile enriched in T cell activation markers. Six clonotypes highly expressed *CD27*, *LTB*, *Lag3*, *Ctla-4*, and *Havcr2* as well as signature genes identified in PD-AML 2 (*Sirpg*, *Ucp2*) (figure 3D). These same six clones highly expressed *Gzmk*, indicating cytolytic capacity. Expanded clones in PD-AML 3 similarly expressed cell-surface PD-1, TIM-3, HLA-DR, and CD27; we noted high 4-1BB expression as well (figure 3E). Again, the clones sharing common DEG and DEP signatures largely exhibited similar magnitudes of expansion in the TCR β -seq data (figure 3F). CD4+ irAE expanded clones also were largely of effector phenotype expressing PD-1, indicative of an activated state (online supplemental figure S6B).

Bulk TCR β -seq allowed evaluation of a large number of T cells from each timepoint (median: 24,181, range: 13,634–31,247) and hence robust identification of novel and expanded T cell clonotypes, which could then be further characterized using scRNA-seq. In contrast however, the use of just a limited number of T cells using scRNA-seq (online supplemental table S8) for discovery of expanded T cell clonotypes would likely lead to false positive results. To demonstrate this, we evaluated T cell clones that were detectable by scRNA-seq at EOC4 but not at earlier time points. For both patients, scRNA-seq identified the majority of clones of interest found with bulk

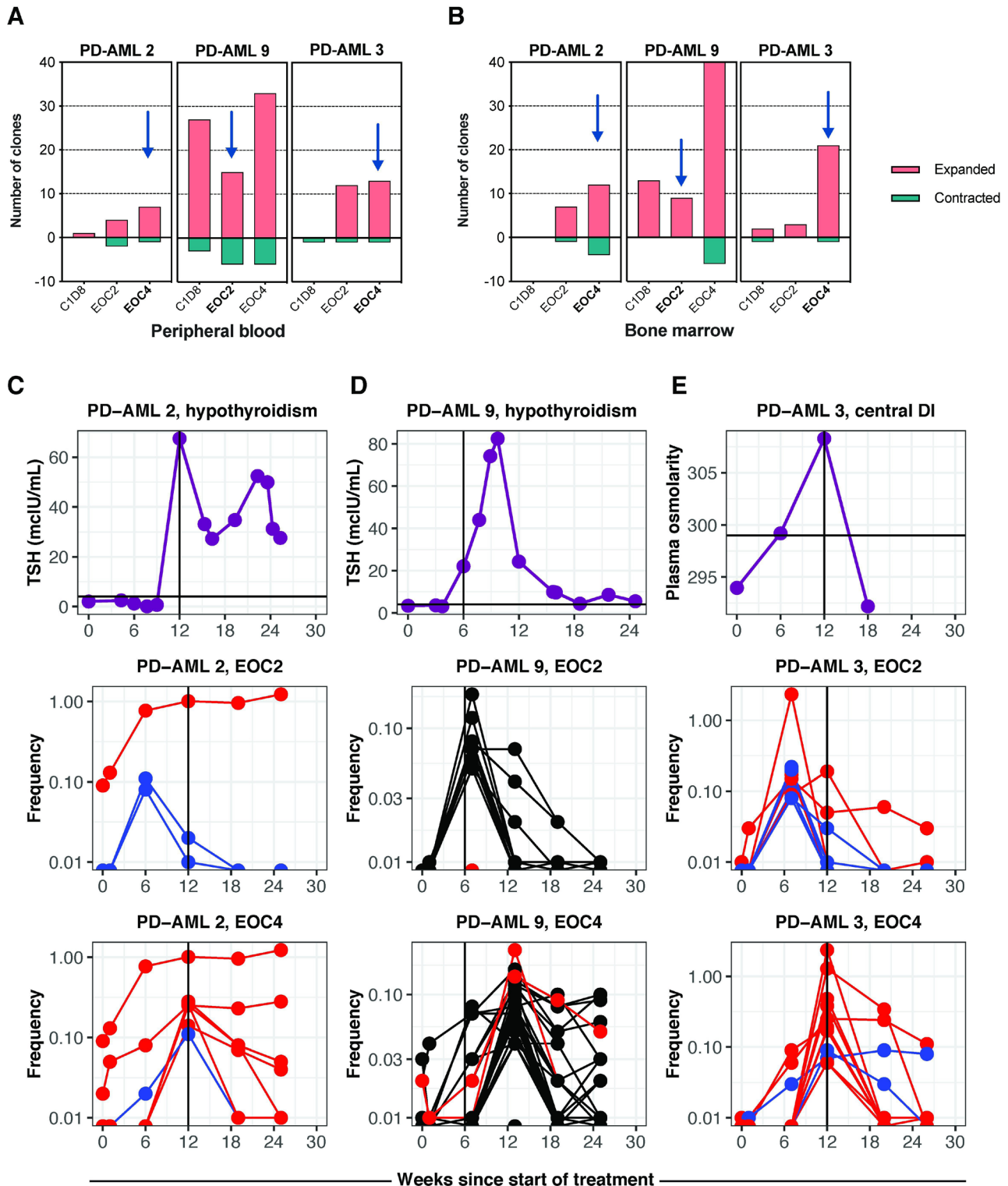


Figure 2 Development of irAEs is associated with clonal T cell expansion. The number of significantly expanded or contracted clones at timepoints sampled during treatment compared to baseline were calculated in (A) peripheral blood (PB) and (B) bone marrow (BM) for patients developing irAEs. Time of irAE indicated by black arrows. TSH levels and significantly expanded T cells at EOC2 and EOC4 in PB that were <0.1% or undetectable at baseline in (C) PD-AML 2, who developed hypothyroidism after 4 cycles of treatment (EOC4, 12 weeks) and (D) PD-AML 9, who developed hypothyroidism after two cycles of treatment (EOC2, 6 weeks). (E) Plasma osmolarity and significantly expanded T cell clones at EOC2 and EOC4 in PB that were <0.1% or undetectable at baseline in PD-AML 3, who developed central diabetes insipidus after 4 cycles of treatment (EOC4, 12 weeks). Upper limit of normal of TSH or plasma osmolarity indicated by black line across y-axes. Each blue, red, or black line represents a unique clonotype for the indicated patient; red indicates CD8⁺ T cell clones, blue indicates CD8⁻ (CD4⁺) T cell clones. Black indicates clones where CD4/CD8 could not be determined. AML, acute myeloid leukemia; irAEs, immune-related adverse events; TSH, thyroid-stimulating hormone.

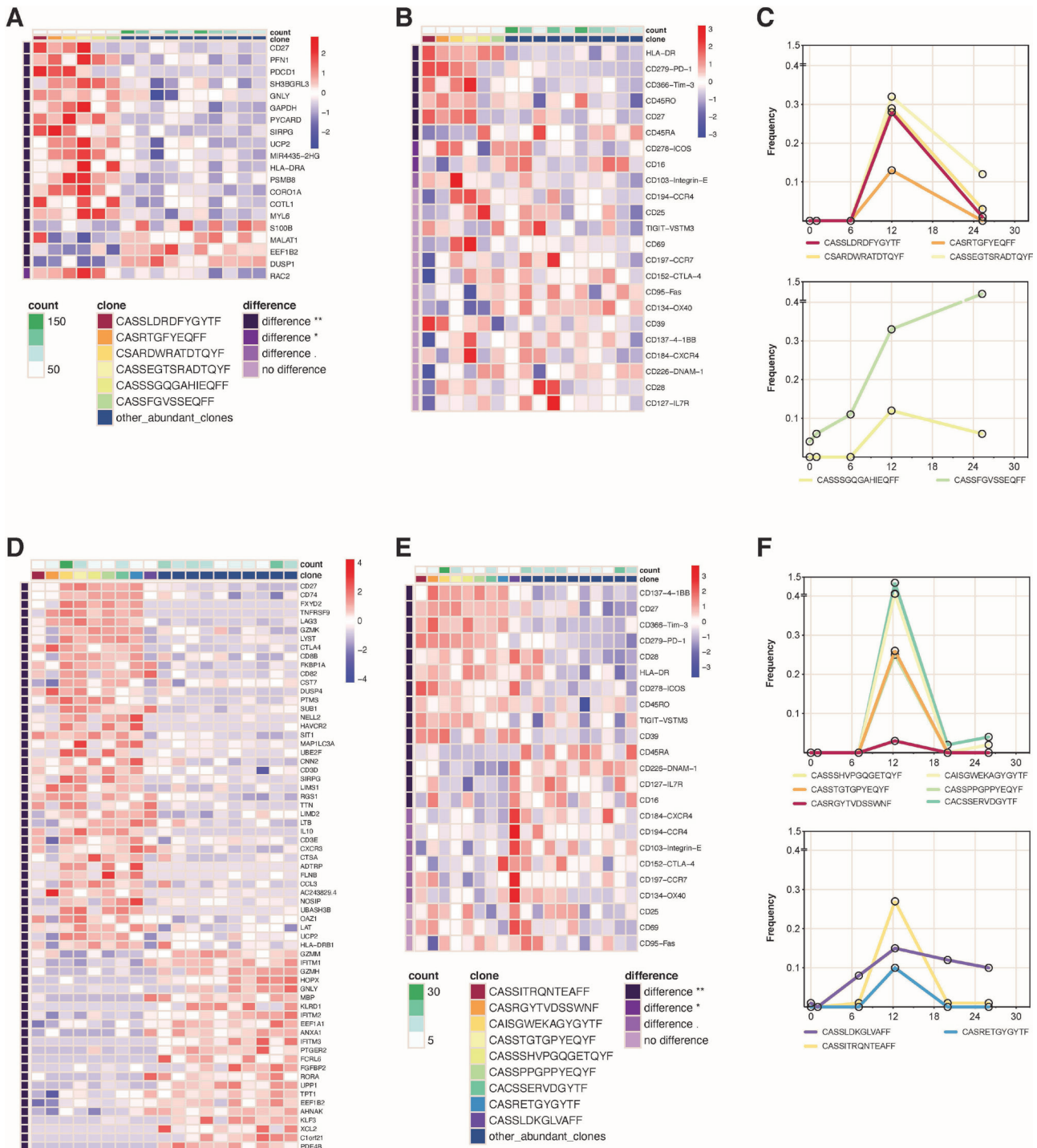


Figure 3 Unique expression signatures in clonally expanded T cells at time of irAE. Cells harboring the unique TCR β CDR3 from differentially abundant clones identified by bulk TCR β -seq were grouped and differentially expressed genes (DEG) and cell surface proteins (DEP) were identified by supervised analyses compared with top 10 abundant T cell clones in the sample identified by bulk TCR β -seq. (A) DEG and (B) DEP of expanded CD8+ T cell clones of interest in PD-AML two at hypothyroidism diagnosis vs other abundant CD8+ T cell clonotypes. (C) Frequencies from TCR β -seq data of clonotypes coexpressing cell surface PD-1, TIM-3, and CD27 (four clones, top panel) and those not expressing this signature (two clones, bottom panel). (D) DEG and (E) DEP of expanded CD8+ T cell clones of interest in PD-AML three at time of diagnosis of central diabetes insipidus versus other abundant CD8+ T cell clonotypes. (F) Frequencies from TCR β -seq data of clonotypes coexpressing cell surface PD-1, TIM-3, 4-1BB, HLA-DR, and CD27 (six clones, top panel) and those not expressing this signature (three clones, bottom panel). Heatmaps were created using the mean expression of all cells within each clone; differentially expressed markers were ordered by adjusted p values and fold changes. Adjusted p values are based on Wilcoxon rank sum test with Bonferroni corrections using all features in the dataset. ‘Difference **’ denotes adjusted $p < 0.01$; ‘difference *’ denotes adjusted $p < 0.05$; ‘difference.’ denotes different but not significantly so. CD8+ T cell clones of interest, expression scale, and significance level are indicated by each heat map. Number of cells in each clone was counted and annotated in green above each heat map.

TCR β -seq with the core PD-1, TIM-3, CD27, and HLA-DR cell surface signature evident (online supplemental figure S6C,D). In addition, however, this scRNA-seq based discovery approach falsely identified clones as emerging at EOC4. Bulk TCR β -seq showed that these clones were most often detectable at baseline or otherwise not significantly expanded, underscoring the limitations of using only scRNA-seq for emerging T cell clone identification (online supplemental figure S6C,D). Downsampling our scRNA-seq datasets to represent experiments performed without pre-enrichment of CD3⁺ cells by flow cytometry exacerbated this issue as the percentage of overlapping clones between two equal-sized samplings of the same patient sample increased as the number of cells sampled increased (online supplemental figure S7A), indicating higher rates of false-positive clone identification with lower cell numbers. Unique clones from the same patient across timepoints also show little overlap no matter how many cells are sampled (online supplemental figure S7B). These data emphasize the importance of acquired T cell number in scRNA-seq experiments as well as the need for statistical definitions of T cell expansions to limit sampling bias and erroneous identification of novel and emerging T cell clonotypes.

Taken together, the use of bulk TCR β -seq to accurately profile clonal dynamics followed by T cell enriched scRNA-seq enabled us to characterize at the gene and protein level these significantly expanded T cell clones at time of irAE, revealing their emergence from a memory into effector phenotype with highly activated and cytotoxic immunogenomic signatures.

Absence of clonal T cell expansions in patients with antileukemic responses

Having identified characteristic signatures associated with induced T cell immune responses in patients developing irAEs during treatment with pembrolizumab and decitabine, we next repeated this analysis for patients experiencing an antileukemic response ('responders'). Surprisingly, and in contrast to the above results for patients with irAEs, bulk TCR β -seq showed that the two patients who completed 24 weeks of therapy and achieved a CR (PD-AML 1 and PD-AML 5) had no significant clonal T cell expansions by EOC4 in either BM or PB (figure 4A,B). We found no characteristic clonal expansion associated with decreasing leukemic disease burden during treatment in either patient (figure 4C,D). PD-AML 1 developed an infection at EOC6, and the CD8⁺ expansions seen at this timepoint likely reflect immune responses to this event (online supplemental figure S8A). For PD-AML 5 at EOC6, 2 differentially expanded CD8⁺ T cell clones were detected that increased in frequency as early as C1D8, although not to statistically significant levels (online supplemental figure S8B). A third responder, PD-AML 10, achieved a MLFS with very hypocellular marrow that precluded reliable estimates of T cell expansions (online supplemental figure S8C). Patients with progressive disease during treatment were either

taken off study early or had few clonal T cell expansions (online supplemental figure S9). As done for longitudinal timepoints in two patients developing irAEs, we performed scRNA-seq on baseline, EOC2, and EOC4 timepoints for two responders PD-AML 1 and PD-AML 5. Despite the limitations of novel T cell clone identification through scRNA-seq discussed earlier, given the absence of significant clonal T cell expansions in these responders, we performed supervised analyses with T cell clones detected at both EOC2 and EOC4 that were not found in earlier timepoints. CD8⁺ T cells in PD-AML 1 at EOC2 and EOC4 that were undetected in prior timepoints by scRNA-seq largely expressed markers indicating activated effector phenotypes, though no shared pattern of PD-1, TIM-3, CD27, and HLA-DR was evident (online supplemental figure S10A). For PD-AML 5 at both EOC2 and EOC4, the number of new T cell clonotypes were so few, identifying meaningful differences compared with previously detected T cell clonotypes was limited (online supplemental figure S10B).

No changes in T cell immunophenotypes and expression profiles in responders during treatment

An alternative hypothesis would be that pembrolizumab would not lead to detectable clonal expansions at the tumor site, but instead would change the activation status of already resident T cell clones. To investigate this possibility, we shifted from clone-driven inquiries to immunophenotype-based analyses. The inclusion of oligonucleotide-labeled antibodies in scRNA-seq allowed for immunophenotyping in a manner analogous to flow cytometry. Using T cell subset-defining markers, we identified CD4⁺ and CD8⁺ naïve, central memory (CM), CD4⁺ CD127^{lo} CD25^{hi} regulatory T cells (Treg), effector memory (EM), and EM re-expressing CD45RA (terminal effectors, TE) T cell populations (figure 5A,B, online supplemental figure S11). Frequencies of CD4⁺ and CD8⁺ T cells derived from scRNA-seq matched well with frequencies calculated from clinical flow cytometry of fresh BM aspirate (online supplemental figure S12A). We confirmed expression of canonical genes that define these given subsets, demonstrating concordance between transcriptional and cell surface expression profiles (figure 5C).

Large changes in frequencies of effector T cell subpopulations were seen in patients developing irAEs, with these patients experiencing at EOC2 36%–59% increases in CD4⁺ EM and an 80% increase in CD8⁺ EM (figure 5D,E). Both patients had 39%–52% increases in CD8⁺ TE at EOC4 as well. Responders maintained stable frequencies of EM populations, though PD-AML 5 experienced over 50% increase in both CD4⁺ and CD8⁺ TE populations by EOC4 (figure 5D,E). Patients developing irAEs had decreases in frequencies of naïve CD4⁺ and CD8⁺ T cells during treatment; all patients had slight decreases in Treg frequencies by EOC4 (online supplemental figure S12B,C). We derived overall sample clonality for T cells sequenced with scRNA-seq, which had

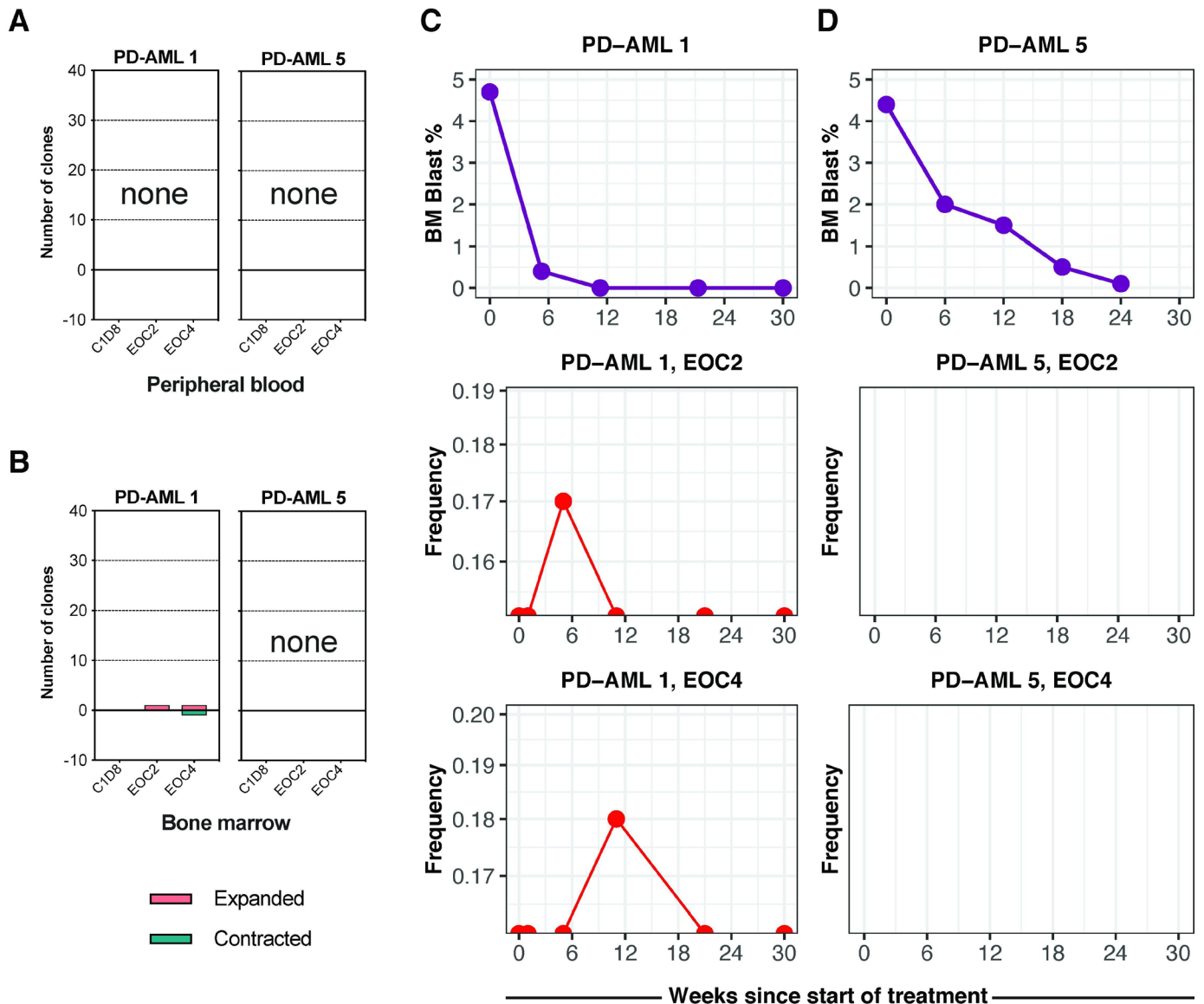


Figure 4 Antileukemic response to combination immunotherapy was not associated with clonal T cell expansion. Number of significantly expanded or contracted clones at timepoints sampled during treatment compared with baseline were calculated in (A) PB and (B) BM for two patients achieving CR by eight cycles of treatment. Decreasing blast percentage in the BM and few to no significantly expanded clones at EOC2 or EOC4 in BM that were low in frequency (<0.1%) or undetectable at baseline in (B) PD-AML one and (C) PD-AML 5. Red lines represent unique CD8⁺ clonotypes.

excellent concordance with bulk clonality values obtained with bulk TCR β -seq (online supplemental figure S12D,E). Our workflow enabled us to compute sample clonality for these specific T cell subsets as well. The increases in CD8⁺ EM frequencies in patients developing irAEs were accompanied by increases in clonality (figure 5F), likely a reflection of the clonal expansions we identified earlier. CD8⁺ TE clonality was also increased in PD-AML 5 at EOC4, suggesting increase in frequency of a more limited number of pre-existing CD8⁺ T cell clones. Overall, however, responders maintained diverse CD4⁺ and CD8⁺ subpopulation TCR β repertoires through EOC4.

The maintenance of high frequency clones that persist from baseline may be associated with response to ICB.⁴⁴ The top 10 most abundant clones identified by TCR β -seq

for all patients at baseline were consistent throughout subsequent sampled timepoints and all fell within CD8⁺ EM and TE clusters (online supplemental figure S13A,B). We next investigated whether the phenotype of these consistently abundant clones changed with treatment. While these abundant clones had differing cell surface profiles from one another, their phenotypes at EOC2 and EOC4 remained unchanged from baseline (online supplemental figure S13C). We also searched for clonotypes in the responders that may have experienced shifts from memory to more effector and/or terminal phenotypes. While we observed heterogeneity in phenotypic composition within clonotypes, the profiles of the clonotypes

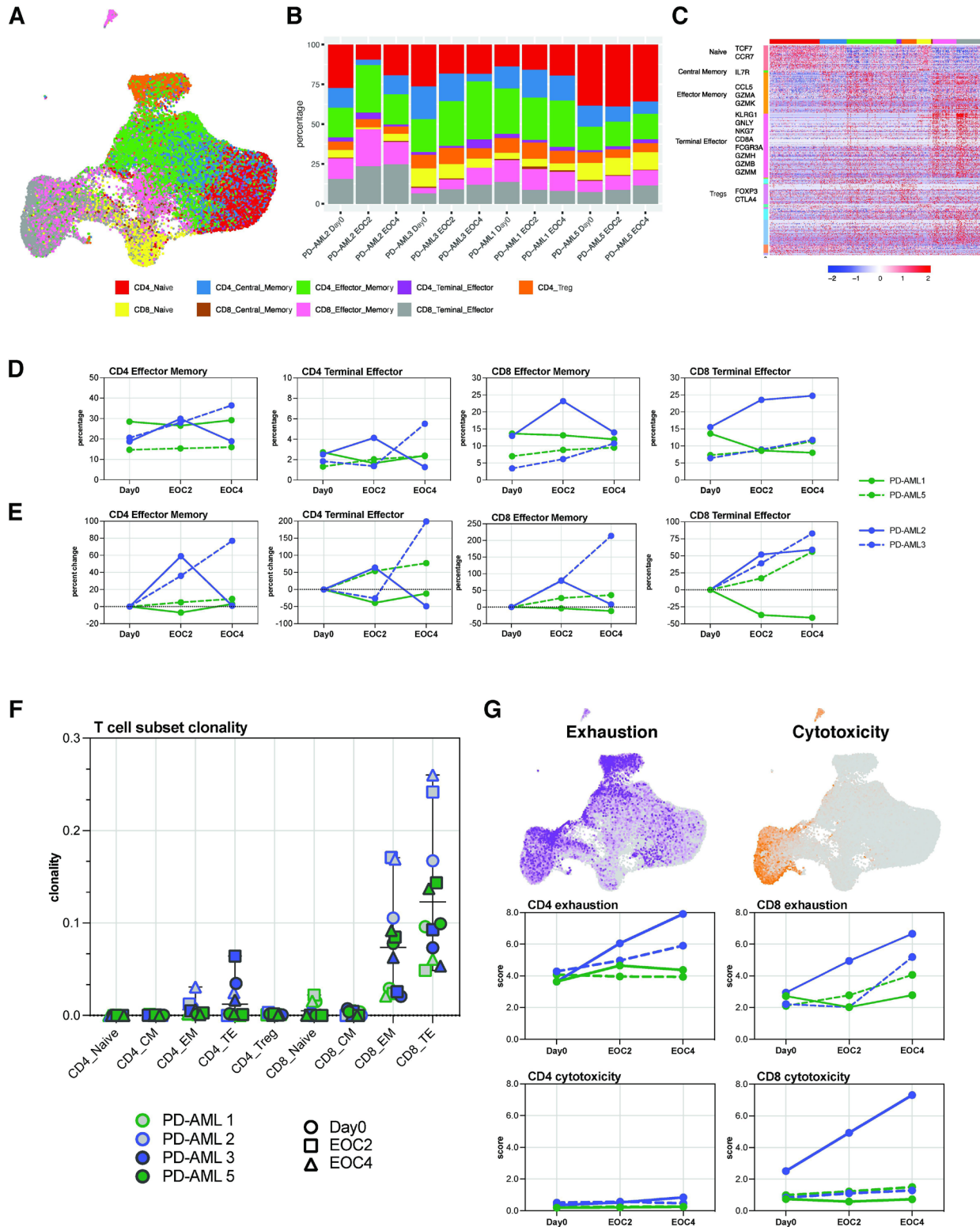


Figure 5 Stable T cell immunophenotypes in patients with anti-leukemic responses. (A) Integrated UMAP visualization of T cell immunophenotyping based on cell surface expression CD4, CD8, CCR7, CD45RA, CD127 and CD25. (B) Quantification and proportion of CD4⁺ and CD8⁺ T cell subset frequencies, as a percentage of CD3⁺. (C) Differential gene expression analysis among different cell types with scaled log normalization. For panels A–C, T cell subsets indicated in legend. (D) Frequencies of CD4⁺ and CD8⁺ effector memory (EM) and terminal effector (TE) T cells at Day0, EOC2, and EOC4. (E) Per cent change in frequencies of CD4⁺ and CD8⁺ EM and TE cells at EOC2 and EOC4 compared with day 0. (F) T cell subset clonality in T cell subsets identified by immunophenotyping. Patients and time points indicated in key. (G) Cells expressing exhaustion (purple) and cytotoxicity (orange) predefined gene sets overlaid on integrated UMAP with exhaustion and cytotoxicity scores for CD4⁺ and CD8⁺ T cells. Scores were calculated for each cell based on mean expression of genes in the gene set and subtracting the background. For panels D–F, individual patients indicated in legend.

at baseline were maintained throughout treatment. We found no clonotype with uniform shifts between T cell phenotypes (online supplemental figure S13D).

Finally, we derived naïve differentiation state, exhaustion, and cytotoxicity scores by computing average scores of gene modules associated with these cell states.⁴⁵ Of note, cells expressing genes within a cytotoxic module were almost exclusively CD8+ effector and TE phenotypes, while cells expressing exhaustion modules consisted of both CD4+ and CD8+ T cell subsets (figure 5G, top). At baseline, all 4 patients had similar CD4+ exhaustion and cytotoxicity scores; at EOC4, patients who developed irAEs had averages of 0.78-fold and 1.31-fold in CD4+ and CD8+ exhaustion scores, respectively (figure 5G). PD-AML 2 also demonstrated a sharp increase in CD8+ cytotoxic state at EOC4; these data are consistent with the clinical development of irAEs at this timepoint in both patients and cellular profiles described earlier. PD-AML 5 demonstrated an increase in CD8+ exhausted state at EOC4, and PD-AML 1 maintained low exhaustion and cytotoxicity scores through treatment (figure 5G). These data suggest increases in aggregate cell cytotoxicity scores are associated with the development of irAEs rather than anti-leukemic response to treatment in these patients.

No evidence of HLA loss in responders at relapse

A third approach to test the hypothesis that anti-PD1 immunotherapy was associated with observed anti-leukemic efficacy is the evaluation for potential immune escape at the time of relapse in those previously responding. Despite continuing maintenance therapy after the completion of this 24-week trial in CR, PD-AML 1 and 5 ultimately both relapsed 374 and 221 days after initiation of protocol treatment, respectively. HLA down-regulation or loss in AML has been reported at relapse after allogeneic transplant.^{46 47} We therefore performed both scRNA-seq and scDNA-seq profiling at baseline and relapse timepoints with unsorted BMMCs from these two patients to evaluate for any evidence of cell-surface HLA loss on the leukemic clone as evidence of immune selective pressure.

Clustering based on cell surface protein expression of scRNA-seq (10x Genomics 3'v3) identified the full array of expected immune cells within each unsorted BM sample (online supplemental figure S14). We focused on populations expressing leukemia-associated immunophenotypes and quantified relative expression of HLA class I and II as well as PD-L1 expression on these putative leukemic clusters. In both patients at relapse, leukemic clusters had stable HLA class I (A, B, C) and class II (DR, DQ, DP) at relapse compared with baseline (figure 6A,B). PD-L1 expression was not increased at relapse for either patient. As use of cell-surface immunophenotype may imperfectly identify leukemic cell populations, we confirmed these findings with an alternative approach. We have previously reported the use of patient-personalized scDNA-seq on baseline samples for these two patients to resolve leukemic clonal landscape.³⁷ We therefore also acquired

scDNA-seq with oligonucleotide-conjugated antibodies against myeloid markers on these relapse samples (figure 6C,D). We confirmed that the relapsing AML had the same genomic mutational features and cell-surface immunophenotype as baseline and that the HLA class I and class II of the leukemic clone remained stable at relapse compared with initial diagnosis.

DISCUSSION

This trial is the first-in-human study of pembrolizumab and decitabine to treat R-AML. We performed integrated multidimensional immunological analysis including longitudinal paired TCR β measurements in PB and BM (ie, the sites of tumor), together with scRNA-seq with full length VDJ TCR sequencing and cell surface antibody-oligonucleotide profiling of isolated T cells to further our understanding of how this immunotherapeutic combination impacts T cell dynamics in R-AML.

While the preclinical rationale for the addition of PD-1 axis ICB to hypomethylating therapy for the treatment of myeloid malignancies is strong,^{21–24} the clinical evidence base for improved efficacy is lacking. One other study to date has published clinical results in R-AML patients treated with a PD-1 inhibitor in conjunction with a HMA,⁴⁸ reporting a response rate (22% CR/CRi) similar both to that observed here and to prior reports of hypomethylating monotherapy in this patient population.^{30 49–53} No clinically meaningful difference in efficacy was noted in a randomized, open-label, international, multicenter study that enrolled untreated myelodysplastic syndrome (MDS) and AML patients to either azacitidine and the anti-PD-L1 agent durvalumab vs azacitidine alone.⁵⁴ Of note, the two patients completing the 24 weeks of planned therapy in CR entered our study with relapsed, low level disease. Currently recruiting randomized studies focus on the addition of pembrolizumab for MRD in combination with either intensive chemotherapy (NCT04214249) or azacitidine and venetoclax (NCT04284787), which will offer better idea of efficacy of ICB for AML particularly in the MRD disease level setting.

Notable clinical events in the present trial were irAEs in 3 (30%) patients, affecting endocrine organs. Meta-analyses suggest that as many as 20% of patients treated with pembrolizumab will develop a thyroid-related autoimmune condition, as was our observation here.⁵⁵ Central diabetes insipidus is a rare irAE affecting the posterior pituitary; one other case of central diabetes insipidus has been reported in a patient treated with the PD-L1 inhibitor avelumab.⁵⁶ A phase I trial of nivolumab as a maintenance therapy post allo-HSCT in patients with AML or MDS (NCT02985554) recently closed early after only 4 patients were treated because of the severe irAEs that occurred in all 4 patients, including one case of hypothyroidism.⁵⁷ The use of nivolumab and ipilimumab either in combination or sequentially is ongoing in AML patients after allo-HSCT (NCT03600155), though no results have been released to date. The relationship between irAE

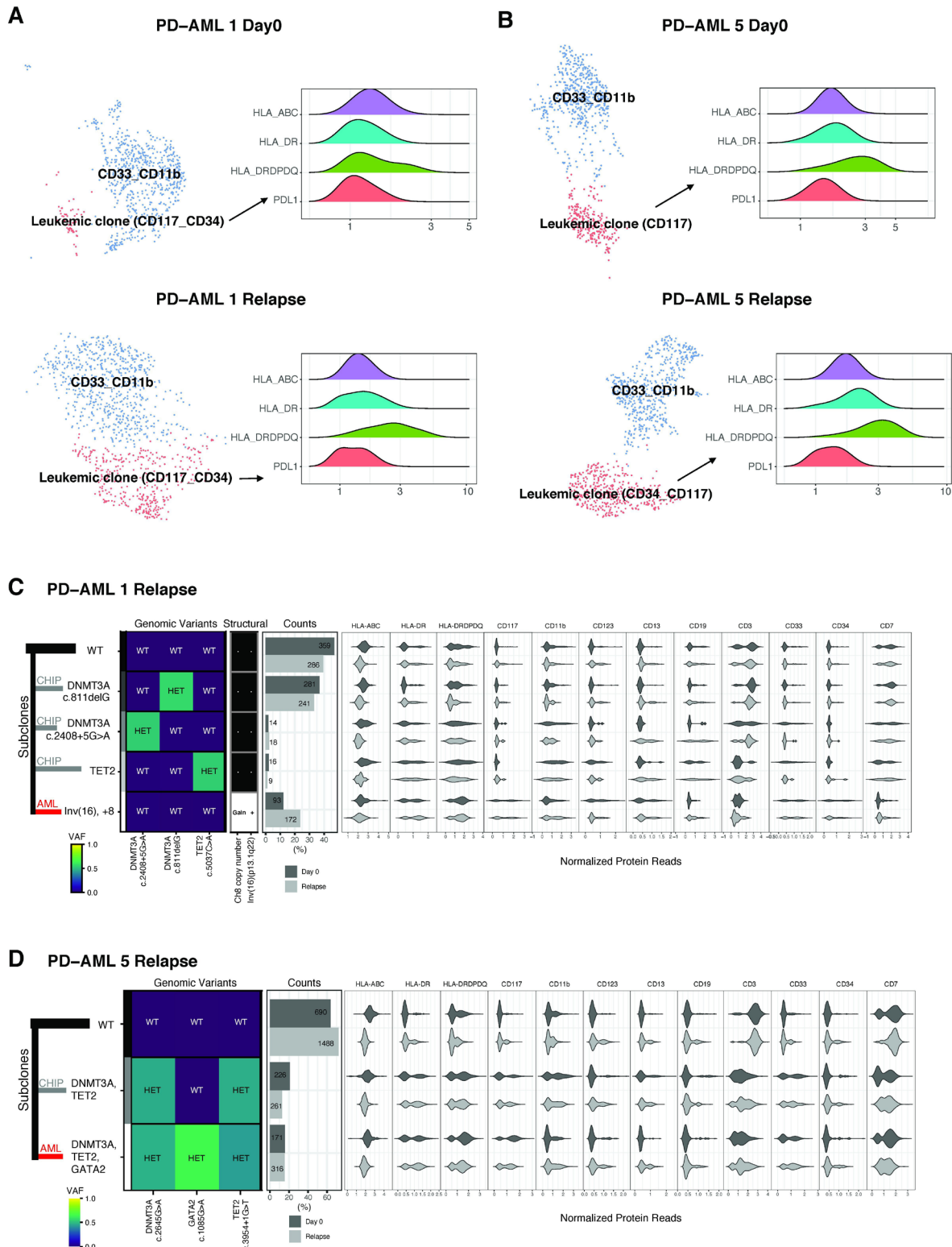


Figure 6 No signal of immune evasion in responders at relapse post-treatment. Through 3'v3 scRNA-seq on unsorted BMBCs, clustering was based on the cell surface protein expression and clusters were annotated by their top three or four most highly differentially expressed markers. Clusters were classified as putative leukemia using on protein expression of known leukemia-associated and myeloid markers based on the patients' previous clinical flow cytometry records. Relative expression of HLA molecules and PD-L1 on leukemic blasts at baseline (top) and at relapse (bottom) in (A) PD-AML 1 and (B) PD-AML 5 visualized using ridge plots. Single-cell DNA and antibody-oligonucleotide sequencing of unsorted BMBCs in (C) PD-AML 1 and (D) PD-AML five shows the genomic and immunophenotypic features of the leukemic (AML, red line) and preceding/distinct CHIP (clonal hematopoiesis, gray lines) clones present at relapse as compared with day 0 (adapted from⁴¹). Left: Genomic subclones with wild type (WT), heterozygous (HET), present (Gain/+) or absent (-) features. Right: Cell surface protein expression for each subclone.

development and anti-tumor response in AML remains unknown.⁵⁸

A key finding of this study comes from the in-depth statistical analyses of specific T cell clonal frequencies during the course of treatment. Differential clonotypic abundance analyses revealed distinctive clonal expansions from previously undetectable levels at the onset/diagnoses of irAEs in three patients treated with pembrolizumab and decitabine. Large numbers of clonal CD8+ T cell expansions preceding the development of grade 2–3 irAEs and early diversification in peripheral TCR β repertoire in patients who ultimately developed irAEs during treatment with ipilimumab have been reported.^{59 60} Our findings differ, as we did not observe broad repertoire shifts in terms of clonality or clonal T cell expansions until a minimum of 6 weeks after pembrolizumab initiation in our R-AML patients developing irAEs. These differences in clonal kinetics may reflect the different mechanisms of actions of anti-CTLA4 and anti-PD-1 drugs.¹¹ Infiltration of memory cytotoxic CD4+ and CD8+ T cells has been identified in ICB-induced encephalitis, and recent single cell studies in patients developing colitis irAEs during ICB identify signatures of proliferation and IFN γ responsiveness in colitis-associated T cells.^{61 62} Our findings of PD-1 and HLA-DR expression on expanded clones of interest are consistent with these reports. We further identify a shared expression module of these two markers as well as TIM-3 and CD27, along with a transcriptional profile indicative of cytotoxicity, cell activation, and co-stimulation in irAE-associated T cells. Based solely on the cell surface co-expression of PD-1 and TIM-3 on these CD8+ T cells, we may have described many of these expanded clones as exhausted or dysfunctional.^{63 64} However, their transcriptional activity and temporal association with irAEs suggest otherwise. Indeed, a strength of our approach is through enrichment of CD3+ T cells for scRNA-seq, which allowed for orthogonal validation and characterization of clones found through bulk TCR β -seq and integration of temporal dynamics with immunogenomics of significantly expanded T cell clones.

Determining immune correlates of antileukemic response in AML patients to ICB is challenging in the absence of randomized clinical trial data.^{65 66} In the current study for two patients who experienced antileukemic benefit during treatment, we intensively scrutinized many CD8+ cellular determinants, including coexpression of inhibitory receptors and activation markers with PD-1, differentiation state of infiltrating T cells with treatment, as well as bystander T cells, all of which have been associated with response to ICB in various solid tumors.^{67–70} However, we found no distinctive changes in these responders and show in fact that instead, changes in these cellular determinants occurred in patients developing irAEs. Moreover, we show here, using the positive control of patients experiencing irAEs clearly attributable to ICB, that assessment of apparently novel or expanded T cell clonotypes by single cell sequencing is subject to sampling bias and false discovery.

The small size of our R-AML cohort is a limitation, as this was a feasibility pilot trial not powered for clinical efficacy assessment. Though some immunomodulatory activities of HMAs on various immune cells have been described, with our trial design, we cannot separate out immunological phenomena caused by pembrolizumab or decitabine alone.^{20 71} Several studies suggest blocking PD-1 may not reinvigorate exhausted and silenced CD8+ T cells due to extensive and non-reversible epigenetic remodeling,^{72 73} though we did not investigate the pretreatment and post-treatment epigenetic landscape in the current study. Future work will investigate the effect of HMAs alone at the single cell level on AML as well as infiltrating and circulating immune cells for better understanding of their immunomodulatory consequences and antileukemic activities. We did not find evidence of T cell-mediated antileukemic responses in the two responders, and the kinetics of clinical response also favor decitabine rather than pembrolizumab as responsible, but we cannot rule out roles of other immune cells. A recent study suggests that response to anti-PD-1 therapy may be dependent on PD-1 expression and signaling in cells of myeloid origin.⁷⁴ The role of myeloid cells in response to ICB is further supported by a study in advanced stage melanoma patients that identified the starting frequency of CD14+ HLA-DRhi monocytes as a strong predictor to response to treatment with anti-PD-1 agents.⁷⁵ Going forward, it will be important to investigate expression of immune checkpoints in non-T cellular compartments in AML both before and during treatment, as their expression on myeloid cells cohabitating with leukemic blasts could influence outcomes during treatment with ICB.

This work is widely relevant to understanding mechanisms behind both irAEs and antitumor responses during ICB. Our methods together uncovered significant expansions of activated EM CD8+ T clones that occurred in a subset of patients developing autoimmune toxicities during treatment with pembrolizumab and decitabine. The combination of immunogenomic signatures and temporal association with irAEs suggest that these clones were previously peripherally silenced and then stimulated during treatment with ICB. Notably, these signatures of T cell expansion and activation were not evident in two patients with R-AML who had anti-leukemic responses to treatment. Our findings contribute to the understanding of immune underpinnings of irAEs induced by ICB and these data serve as a valuable resource for examining the effects of pembrolizumab and decitabine in combination on T cell dynamics in AML at the single cell level.

Author affiliations

¹National Heart Lung and Blood Institute, Bethesda, Maryland, USA

²National Cancer Institute, Bethesda, Maryland, USA

³Center for Drug Evaluation and Research, Food and Drug Administration, Silver Spring, Maryland, USA

⁴National Institutes of Health Clinical Center, Bethesda, Maryland, USA

⁵National Institute of Diabetes and Digestive and Kidney Diseases, Bethesda, Maryland, USA

⁶Trans-NIH Center for Human Immunology, National Institutes of Health, Bethesda, Maryland, USA

Twitter James L Gullejy @gullejy1 and Christopher S Hourigan @DrChrisHourigan

Acknowledgements We appreciate the technical expertise of the NHLBI Flow Cytometry and DNA Sequencing Cores. Thank you to Steven Soldin (NIH Clinical Center) for technical guidance. We thank the NIH HPC Biowulf cluster for their computational resources (<http://hpc.nih.gov>). This work is supported in part by a research grant from Investigator-Initiated Studies Program of Merck Sharp & Dohme.

Contributors MG, GG, LWD and CSH wrote the manuscript. MG, GG and LWD made the figures. MG, LWD, KEL, JYG, KAO, YL, PD, JLM, JdR, JK-G, JLG and CSH designed experiments. MG, LWD, KEL and PD performed experiments. MG, GG, LWD, D-YK, KAO, KRC and CSH analyzed and interpreted data. JT, JV, KAO, CBD, TH, KRC, CL and CSH were involved in the clinical care of the patients. DMS, HT, CL and CHS developed the clinical concept and design CSH supervised the study. CSH is the guarantor of this work. All authors reviewed and approved the final manuscript.

Funding This work was supported by the Intramural Research Program of the National Heart, Lung, and Blood Institute (NHLBI) of the National Institutes of Health (NIH), a Cooperative Research and Development Agreement with Merck Sharpe & Dohme, and by funding from the trans-NIH Center for Human Immunology.

Disclaimer The opinions expressed in this paper are those of the authors and do not necessarily represent those of Merck Sharp & Dohme.

Competing interests CSH receives research support from Merck Sharpe & Dohme and SELLAS Life Sciences Group AG. CL is on the Speakers' Bureau for Astellas, Jazz Pharma and serves in a consulting or advisory role for Daiichi, Jazz Pharma, Amgen, Abbvie, MacroGenics, and Agios. The remaining authors declare no competing interests.

Patient consent for publication Not applicable.

Ethics approval 17-H-0026, (PD-AML, NCT02996474) was an investigator sponsored, single-institution, single-arm open-label 10 subject study approved by the NHLBI IRB and conducted in accordance with the Declaration of Helsinki (FDA IND: 131826).

Provenance and peer review Not commissioned; externally peer reviewed.

Data availability statement Data are available in a public, open access repository. Data are available on reasonable request. Bulk TCR β sequencing data are available on the ImmunoSEQ Analyzer through AdaptiveBiotechnologies. scRNA-seq data sets are available through the National Center for Biotechnology Information's Gene Expression Omnibus. Code available on request.

Supplemental material This content has been supplied by the author(s). It has not been vetted by BMJ Publishing Group Limited (BMJ) and may not have been peer-reviewed. Any opinions or recommendations discussed are solely those of the author(s) and are not endorsed by BMJ. BMJ disclaims all liability and responsibility arising from any reliance placed on the content. Where the content includes any translated material, BMJ does not warrant the accuracy and reliability of the translations (including but not limited to local regulations, clinical guidelines, terminology, drug names and drug dosages), and is not responsible for any error and/or omissions arising from translation and adaptation or otherwise.

Open access This is an open access article distributed in accordance with the Creative Commons Attribution 4.0 Unported (CC BY 4.0) license, which permits others to copy, redistribute, remix, transform and build upon this work for any purpose, provided the original work is properly cited, a link to the licence is given, and indication of whether changes were made. See <https://creativecommons.org/licenses/by/4.0/>.

ORCID iDs

Jack Y Ghannam <http://orcid.org/0000-0003-0275-9099>

James L Gullejy <http://orcid.org/0000-0002-6569-2912>

Christopher S Hourigan <http://orcid.org/0000-0002-6189-8067>

REFERENCES

- Breems DA, Van Putten WLJ, Huijgens PC, *et al.* Prognostic index for adult patients with acute myeloid leukemia in first relapse. *J Clin Oncol* 2005;23:1969–78.
- Ramos NR, Mo CC, Karp JE, *et al.* Current approaches in the treatment of relapsed and refractory acute myeloid leukemia. *J Clin Med* 2015;4:665–95.
- Ferrara JLM, Levine JE, Reddy P, *et al.* Graft-versus-host disease. *Lancet* 2009;373:1550–61.
- van Bergen CAM, van Luxemburg-Heijs SAP, de Wreede LC, *et al.* Selective graft-versus-leukemia depends on magnitude and diversity of the alloreactive T cell response. *J Clin Invest* 2017;127:517–29.
- Ribas A, Wolchok JD. Cancer immunotherapy using checkpoint blockade. *Science* 2018;359:1350–5.
- Mueller SN, Ahmed R. High antigen levels are the cause of T cell exhaustion during chronic viral infection. *Proc Natl Acad Sci U S A* 2009;106:8623–8.
- Wherry EJ, Blattman JN, Murali-Krishna K, *et al.* Viral persistence alters CD8 T-cell immunodominance and tissue distribution and results in distinct stages of functional impairment. *J Virol* 2003;77:4911–27.
- Topalian SL, Hodi FS, Brahmer JR, *et al.* Safety, activity, and immune correlates of anti-PD-1 antibody in cancer. *N Engl J Med* 2012;366:2443–54.
- Hamid O, Robert C, Daud A, *et al.* Safety and tumor responses with lambrolizumab (anti-PD-1) in melanoma. *N Engl J Med* 2013;369:134–44.
- Barber DL, Wherry EJ, Masopust D, *et al.* Restoring function in exhausted CD8 T cells during chronic viral infection. *Nature* 2006;439:682–7.
- Wei SC, Duffy CR, Allison JP. Fundamental mechanisms of immune checkpoint blockade therapy. *Cancer Discov* 2018;8:1069–86.
- Zhang L, Gajewski TF, Kline J. PD-1/PD-L1 interactions inhibit antitumor immune responses in a murine acute myeloid leukemia model. *Blood* 2009;114:1545–52.
- Zhou Q, Munger ME, Highfill SL, *et al.* Program death-1 signaling and regulatory T cells collaborate to resist the function of adoptively transferred cytotoxic T lymphocytes in advanced acute myeloid leukemia. *Blood* 2010;116:2484–93.
- Goswami M, Lindblad KE, Ramraj R, *et al.* B cell deficiency in patients with relapsed and refractory acute myeloid leukemia. *Clin Hematol Int* 2020;2:125–8.
- Williams P, Basu S, Garcia-Manero G, *et al.* The distribution of T-cell subsets and the expression of immune checkpoint receptors and ligands in patients with newly diagnosed and relapsed acute myeloid leukemia. *Cancer* 2019;125:1470–81.
- Jia B, Wang L, Claxton DF, *et al.* Bone marrow CD8 T cells express high frequency of PD-1 and exhibit reduced anti-leukemia response in newly diagnosed AML patients. *Blood Cancer J* 2018;8:34.
- Le Dieu R, Taussig DC, Ramsay AG, *et al.* Peripheral blood T cells in acute myeloid leukemia (AML) patients at diagnosis have abnormal phenotype and genotype and form defective immune synapses with AML blasts. *Blood* 2009;114:3909–16.
- Knaus HA, Berglund S, Hackl H, *et al.* Signatures of CD8+ T cell dysfunction in AML patients and their reversibility with response to chemotherapy. *JCI Insight* 2018;3 doi:10.1172/jci.insight.120974
- Schnorfeil FM, Lichtenegger FS, Emmerig K, *et al.* T cells are functionally not impaired in AML: increased PD-1 expression is only seen at time of relapse and correlates with a shift towards the memory T cell compartment. *J Hematol Oncol* 2015;8:93.
- Lindblad KE, Goswami M, Hourigan CS, *et al.* Immunological effects of hypomethylating agents. *Expert Rev Hematol* 2017;10:745–52.
- Yang H, Bueso-Ramos C, DiNardo C, *et al.* Expression of PD-L1, PD-L2, PD-1 and CTLA4 in myelodysplastic syndromes is enhanced by treatment with hypomethylating agents. *Leukemia* 2014;28:1280–8.
- Ørskov AD, Treppendahl MB, Skovbo A, *et al.* Hypomethylation and up-regulation of PD-1 in T cells by azacitidine in MDS/AML patients: a rationale for combined targeting of PD-1 and DNA methylation. *Oncotarget* 2015;6:9612–26.
- Goodyear O, Agathangelou A, Novitzky-Basso I, *et al.* Induction of a CD8+ T-cell response to the MAGE cancer testis antigen by combined treatment with azacitidine and sodium valproate in patients with acute myeloid leukemia and myelodysplasia. *Blood* 2010;116:1908–18.
- Srivastava P, Paluch BE, Matsuzaki J, *et al.* Induction of cancer testis antigen expression in circulating acute myeloid leukemia blasts following hypomethylating agent monotherapy. *Oncotarget* 2016;7:12840–56.
- Chiappinelli KB, Strissel PL, Desrichard A, *et al.* Inhibiting DNA methylation causes an interferon response in cancer via dsRNA including endogenous retroviruses. *Cell* 2015;162:974–86.
- Roulois D, Loo Yau H, Singhania R, *et al.* DNA-Demethylating agents target colorectal cancer cells by inducing viral mimicry by endogenous transcripts. *Cell* 2015;162:961–73.
- Jiang TT, Martinov T, Xin L, *et al.* Programmed Death-1 Culls Peripheral Accumulation of High-Affinity Autoreactive CD4 T Cells to Protect against Autoimmunity. *Cell Rep* 2016;17:1783–94.

- 28 Francisco LM, Sage PT, Sharpe AH. The PD-1 pathway in tolerance and autoimmunity. *Immunol Rev* 2010;236:219–42.
- 29 Tallman MS, Wang ES, Altman JK, et al. Acute myeloid leukemia, version 3.2019, NCCN clinical practice guidelines in oncology. *J Natl Compr Canc Netw* 2019;17:721–749.
- 30 Welch JS, Petti AA, Miller CA, et al. TP53 and decitabine in acute myeloid leukemia and myelodysplastic syndromes. *N Engl J Med* 2016;375:2023–36.
- 31 Oetjen KA, Lindblad KE, Goswami M, et al. Human bone marrow assessment by single-cell RNA sequencing, mass cytometry, and flow cytometry. *JCI Insight* 2018;3 doi:10.1172/jci.insight.124928
- 32 Carlson CS, Emerson RO, Sherwood AM, et al. Using synthetic templates to design an unbiased multiplex PCR assay. *Nat Commun* 2013;4:2680.
- 33 Robins HS, Campregher PV, Srivastava SK, et al. Comprehensive assessment of T-cell receptor beta-chain diversity in alphabeta T cells. *Blood* 2009;114:4099–107.
- 34 Lefranc M-P, Giudicelli V, Ginestoux C, et al. IMGT, the International immunogenetics information system. *Nucleic Acids Res* 2009;37:D1006–12.
- 35 DeWitt WS, Emerson RO, Lindau P, et al. Dynamics of the cytotoxic T cell response to a model of acute viral infection. *J Virol* 2015;89:4517–26.
- 36 Rytlewski J, Deng S, Xie T, et al. Model to improve specificity for identification of clinically-relevant expanded T cells in peripheral blood. *PLoS One* 2019;14:e0213684.
- 37 Dillon LW, Ghannam J, Nosiri C, et al. Personalized single-cell Proteogenomics to distinguish acute myeloid leukemia from non-malignant clonal hematopoiesis. *Blood Cancer Discov* 2021;2:319–25.
- 38 Hopkins AC, Yarchoan M, Durham JN, et al. T cell receptor repertoire features associated with survival in immunotherapy-treated pancreatic ductal adenocarcinoma. *JCI Insight* 2018;3 doi:10.1172/jci.insight.122092
- 39 Hogan SA, Courtier A, Cheng PF, et al. Peripheral blood TCR repertoire profiling may facilitate patient stratification for immunotherapy against melanoma. *Cancer Immunol Res* 2019;7:77–85.
- 40 Lee H, Hodi FS, Giobbie-Hurder A, et al. Characterization of thyroid disorders in patients receiving immune checkpoint inhibition therapy. *Cancer Immunol Res* 2017;5:1133–40.
- 41 de Filette J, Jansen Y, Schreuer M, et al. Incidence of thyroid-related adverse events in melanoma patients treated with pembrolizumab. *J Clin Endocrinol Metab* 2016;101:4431–9.
- 42 McLachlan SM, Rapoport B. Breaking tolerance to thyroid antigens: changing concepts in thyroid autoimmunity. *Endocr Rev* 2014;35:59–105.
- 43 Cohen NR, Brennan PJ, Shay T, et al. Shared and distinct transcriptional programs underlie the hybrid nature of iNKT cells. *Nat Immunol* 2013;14:90–9.
- 44 Cha E et al. Improved survival with T cell clonotype stability after anti-CTLA-4 treatment in cancer patients. *Sci Transl Med* 2014;6:ra270.
- 45 Zhang J-Y, Wang X-M, Xing X, et al. Single-Cell landscape of immunological responses in patients with COVID-19. *Nat Immunol* 2020;21:1107–18.
- 46 Christopher MJ, Petti AA, Rettig MP, et al. Immune escape of relapsed AML cells after allogeneic transplantation. *N Engl J Med* 2018;379:2330–41.
- 47 Vago L, Perna SK, Zanussi M, et al. Loss of mismatched HLA in leukemia after stem-cell transplantation. *N Engl J Med* 2009;361:478–88.
- 48 Daver N, Garcia-Manero G, Basu S, et al. Efficacy, safety, and biomarkers of response to azacitidine and nivolumab in relapsed/refractory acute myeloid leukemia: a nonrandomized, open-label, phase II study. *Cancer Discov* 2019;9:370–83.
- 49 Ritchie EK, Feldman EJ, Christos PJ, et al. Decitabine in patients with newly diagnosed and relapsed acute myeloid leukemia. *Leuk Lymphoma* 2013;54:2003–7.
- 50 Khan N, Hantel A, Knoebel RW, et al. Efficacy of single-agent decitabine in relapsed and refractory acute myeloid leukemia. *Leuk Lymphoma* 2017;58:1–7.
- 51 Bouligny IM, Mehta V, Isom S, et al. Efficacy of 10-day decitabine in acute myeloid leukemia. *Leuk Res* 2021;103:106524.
- 52 Lessi F, Laurino M, Papayannidis C, et al. Hypomethylating agents (HMAs) as salvage therapy in relapsed or refractory AML: an Italian multicentric retrospective study. *Biomedicines* 2021;9. doi:10.3390/biomedicines9080972. [Epub ahead of print: 06 08 2021].
- 53 Stahl M, DeVeaux M, Montesinos P, et al. Hypomethylating agents in relapsed and refractory AML: outcomes and their predictors in a large international patient cohort. *Blood Adv* 2018;2:923–32.
- 54 Zeidan AM, Cavenagh J, Voso MT, et al. Efficacy and safety of azacitidine (aza) in combination with the anti-PD-L1 Durvalumab (durva) for the front-line treatment of older patients (PTS) with acute myeloid leukemia (AML) who are unfit for intensive chemotherapy (IC) and PTS with higher-risk myelodysplastic syndromes (HR-MDS): results from a large, international, randomized phase 2 study. *Blood* 2019;134:829. doi:10.1182/blood-2019-122896
- 55 Barroso-Sousa R, Barry WT, Garrido-Castro AC, et al. Incidence of endocrine dysfunction following the use of different immune checkpoint inhibitor regimens: a systematic review and meta-analysis. *JAMA Oncol* 2018;4:173–82.
- 56 Zhao C, Tella SH, Del Rivero J, et al. Anti-PD-L1 treatment induced central diabetes insipidus. *J Clin Endocrinol Metab* 2018;103:365–9.
- 57 Wang AY, Kline J, Stock W, et al. Unexpected toxicities when nivolumab was given as maintenance therapy following allogeneic stem cell transplantation. *Biol Blood Marrow Transplant* 2020;26:1025–7.
- 58 Gesiotto QJ, Swoboda DM, Shallis RM, et al. Evaluating predictors of immune-related adverse events and response to checkpoint inhibitors in myeloid malignancies. *Clin Lymphoma Myeloma Leuk* 2021;21:421–4.
- 59 Oh DY, Cham J, Zhang L, et al. Immune toxicities Elicited by CTLA-4 blockade in cancer patients are associated with early diversification of the T-cell repertoire. *Cancer Res* 2017;77:1322–30.
- 60 Subudhi SK, Aparicio A, Gao J, et al. Clonal expansion of CD8 T cells in the systemic circulation precedes development of ipilimumab-induced toxicities. *Proc Natl Acad Sci U S A* 2016;113:11919–24.
- 61 Luoma AM, Suo S, Williams HL, et al. Molecular pathways of colon inflammation induced by cancer immunotherapy. *Cell* 2020;182:655–71.
- 62 Johnson DB, McDonnell WJ, Gonzalez-Ericsson PI, et al. A case report of clonal EBV-like memory CD4⁺ T cell activation in fatal checkpoint inhibitor-induced encephalitis. *Nat Med* 2019;25:1243–50.
- 63 Kong Y, Zhang J, Claxton DF, et al. PD-1(hi)TIM-3(+) T cells associate with and predict leukemia relapse in AML patients post allogeneic stem cell transplantation. *Blood Cancer J* 2015;5:e330.
- 64 Blackburn SD, Shin H, Haining WN, et al. Coregulation of CD8⁺ T cell exhaustion by multiple inhibitory receptors during chronic viral infection. *Nat Immunol* 2009;10:29–37.
- 65 Vadakekolathu J, Minden MD, Hood T, et al. Immune landscapes predict chemotherapy resistance and immunotherapy response in acute myeloid leukemia. *Sci Transl Med* 2020;12 doi:10.1126/scitranslmed.aaz0463
- 66 Abbas HA et al. Single-cell characterization of acute myeloid leukemia and its microenvironment following PD-1 blockade based therapy. *Biorxiv* 2020.
- 67 Kurtulus S, Madi A, Escobar G, et al. Checkpoint blockade immunotherapy induces dynamic changes in PD¹CD8⁺ tumor-infiltrating T cells. *Immunity* 2019;50:181–94.
- 68 Yost KE, Satpathy AT, Wells DK, et al. Clonal replacement of tumor-specific T cells following PD-1 blockade. *Nat Med* 2019;25:1251–9.
- 69 Miller BC, Sen DR, Al Abosy R, et al. Subsets of exhausted CD8⁺ T cells differentially mediate tumor control and respond to checkpoint blockade. *Nat Immunol* 2019;20:326–36.
- 70 Thommen DS, Koelzer VH, Herzig P, et al. A transcriptionally and functionally distinct PD-1⁺ CD8⁺ T cell pool with predictive potential in non-small-cell lung cancer treated with PD-1 blockade. *Nat Med* 2018;24:994–1004.
- 71 Daver N, Boddu P, Garcia-Manero G, et al. Hypomethylating agents in combination with immune checkpoint inhibitors in acute myeloid leukemia and myelodysplastic syndromes. *Leukemia* 2018;32:1094–105.
- 72 Ghoneim HE, Fan Y, Moustaki A, et al. De novo epigenetic programs inhibit PD-1 blockade-mediated T cell rejuvenation. *Cell* 2017;170:142–57.
- 73 Pauken KE, Sammons MA, Odorizzi PM, et al. Epigenetic stability of exhausted T cells limits durability of reinvigoration by PD-1 blockade. *Science* 2016;354:1160–5.
- 74 Strauss L, Mahmoud MAA, Weaver JD, et al. Targeted deletion of PD-1 in myeloid cells induces antitumor immunity. *Sci Immunol* 2020;5:1. doi:10.1126/sciimmunol.aay1863
- 75 Krieg C, Nowicka M, Guglietta S, et al. High-dimensional single-cell analysis predicts response to anti-PD-1 immunotherapy. *Nat Med* 2018;24:144–53.
- 76 Çelik H, Lindblad KE, Popescu B, et al. Highly multiplexed proteomic assessment of human bone marrow in acute myeloid leukemia. *Blood Adv* 2020;4:367–79.